Int. J. Heat Mass Transfer. Vol. 30, No. 11, pp. 2385–2397, 1987
Printed in Great Britain

0017 9310/87 $3.00 + 0.00

Heat transfer and two-phase flow during convective boiling in a partially-heated cross-ribbed channel

X. XU and V. P. CAREY
Department of Mechanical Engineering, University of California, Berkeley, CA 94720, U.S.A.

(*Received* 18 *August* 1986 *and in final form* 21 *April* 1987)

Abstract—Measured local heat transfer data and visual observations of the two-phase flow behavior are reported for convective boiling of saturated liquids in a cross-ribbed channel similar to geometries used in formed-plate compact heat exchangers. Experiments in this study were conducted using a special test section which permitted direct visual observation of the boiling process while simultaneously measuring the local heat transfer coefficient at several locations along the channel. One wall of the channel was heated while the opposite and lateral walls were adiabatic. Measured local heat transfer coefficients on the heated portion of the channel wall were obtained for convective boiling of methanol and n-butanol at atmospheric pressure with the channel oriented vertically and in horizontal positions with top heating, side heating and bottom heating of the channel. Vertical flows were observed to be in the churn or annular flow regimes over most of the channel length whereas the horizontal flows were either in the wavy or annular flow regime over most of the channel. Visual observations also indicated that virtually no nucleate boiling was present when the flow was in one of these three regimes. For the same coolant and flow conditions, at moderate to high qualities, the measured convective boiling heat transfer coefficients for the vertical and horizontal orientations were usually found to differ by only a small amount. However, for some orientations, partial dryout of the heated wall of the channel was sometimes observed to reduce the heat transfer coefficient. A method of correlating the heat transfer data for annular film-flow boiling in cross-ribbed channel geometries is also described.

INTRODUCTION

RIBBED-plate heat exchangers have been widely used in the chemical and food processing industries and in aerospace and automotive applications for many years. Manufacturers of heat exchangers with ribbed-plate geometries include Alfal Laval, Bavex, Inc., APV Company, the Paul Mueller Company, and General Motors. Because the ribbed walls of formed-plate heat exchangers act to turbulate the flow, the heat transfer coefficient in the ribbed-wall channels is typically much higher than that for a round tube under comparable conditions. Consequently, a smaller, lighter ribbed-plate heat exchanger may often do the job of a larger, heavier tube and shell unit. Ribbed-plate heat exchangers are commonly used for liquid–liquid heat transfer, and are sometimes used in applications involving gas–gas or gas–liquid heat transfer.

In addition to their use for single-phase applications, units of this type have also seen limited use as evaporators in process heat transfer applications in the chemical and petroleum industries. Ribbed-plate channels have also been used in compact brazed aluminum evaporators for automotive air-conditioning systems manufactured by General Motors. Ribbed-plate heat exchangers have also been considered for evaporator applications in Ocean Thermal Energy Conversion (OTEC) systems.

Despite their potential use in the applications noted above, little information on the convective boiling performance of cross-ribbed channel geometries is available in the open literature. A number of previous studies have investigated flow boiling heat transfer in tubes or channels with walls having ribs oriented parallel or transverse to the flow (see, e.g. refs. [1–3]). However, the geometries used in the ribbed-plate heat exchangers described above are unlike any of the rib configurations considered in these studies.

In ribbed-plate heat exchangers, the ribs are often oriented at an angle between 20° and 70° to the flow direction. In addition, the rib pattern is usually designed so that the ribs on the opposite wall of the channel are oriented at a different angle, and so that ribs on opposite walls touch at locations where they cross. This results in a very complex geometry which forces the flow to twist and turn as it passes through the channel. The flow behavior in these geometries is expected to be much different than that in tubes or channels with parallel or transverse ribs along the walls. Consequently, the results of the studies mentioned above are not expected to apply to the cross-ribbed geometries of interest here.

The convective boiling heat transfer performance of several different ribbed-plate heat exchangers has been determined experimentally in a recent study by Panchal *et al.* [4] at Argonne National Laboratory. These units were evaluated for use as evaporators in a proposed OTEC system. Ribbed-plate heat

NOMENCLATURE

A	constant in equation (4)
A_R	surface area of ribs in channel section of length L_c
A_p	prime surface area of channel section of length L_c
A_0	cross-sectional open area of channel
c_p	specific heat at constant pressure
d_h	hydraulic diameter based on wetted perimeter, $4A_0/P_W$
d_{hp}	hydraulic diameter based on heated perimeter, $4A_0/P_H$
f	friction factor
F	flow regime parameter, $[\rho_g j_g^2/(\rho_f-\rho_g)d_h g]^{1/2}$
G	mass flux
h	heat transfer coefficient
H	dimension of ribs from root to tip
j_f	volume flux of liquid, $G(1-x)/\rho_f$
j_g	volume flux of vapor, Gx/ρ_g
j_g^*	dimensionless volume flux of vapor, $j_g\rho_g^{1/2}[gd_h(\rho_f-\rho_g)]^{-1/2}$
k	fluid thermal conductivity
k_c	conductivity of copper
K	flow regime parameter, $[\rho_g j_g^2 j_f/(\rho_f-\rho_g)g\nu_f]^{1/2}$
L_c	length of channel section
n	exponent in equation (4)
p	pressure
P_H	heated perimeter
P_W	wetted perimeter
Pr_f	liquid Prandtl number
q''	surface heat flux
Re_f	liquid Reynolds number, $G(1-x)d_h/\mu_f$
Re_g	vapor Reynolds number, Gxd_h/μ_g
Re_{fp}	liquid Reynolds number based on heated perimeter, $G(1-x)d_{hp}/\mu_f$
St	Stanton number, h/Gc_p
t	rib thickness
T_W	wall temperature of prime surface of channel
T_M	bulk mean temperature of the coolant
T_{SAT}	saturation temperature of coolant
W_c	width of copper slab
x	mass quality
X_{tt}	Martinelli parameter for turbulent–turbulent flow, $[(dp/dz)_{Ff}/(dp/dz)_{Fg}]^{1/2}$.

Greek symbols

μ	absolute viscosity
ν	kinematic viscosity
Ψ	parameter defined in equation (3).

Subscripts

f	liquid properties or corresponding to liquid flow alone in the channel
g	vapor properties or corresponding to vapor flow alone in the channel
fp	corresponding to liquid flow alone in the channel heated on one side only
F	friction component of pressure gradient
tp	corresponding to two-phase flow conditions.

exchangers manufactured by Tranter and Alpha Laval were tested with the channels oriented vertically using ammonia or R-22 as the working fluid.

These tests provided performance data for three different rib geometries over a wide range of operating conditions. However, only overall performance of the unit is reported in ref. [4]. From the reported data it is not possible to determine the heat transfer coefficient (either local or mean) on the boiling side of the unit. The authors did conclude that the mode of boiling heat transfer seems to consist of nucleate boiling as well as forced-convection evaporation. They expected nucleate boiling to be dominant in the lower part of the heat exchanger, and forced-convection evaporation was expected to become important in the upper part of the unit.

The studies described above provide very little information about convective boiling and two-phase flow in cross-ribbed channel geometries. The results of many previous studies of flow boiling heat transfer in tubes or channels with ribbed walls do not apply to the cross-ribbed channel geometries considered here because the geometries are very different. The study of Panchal *et al.* [4] provides some insight into the performance of cross-ribbed channel geometries in evaporator applications. However, only very limited conclusions about the boiling mechanism can be made from the overall heat transfer measurements made in this study.

In addition, data obtained by manufacturers of ribbed-plate heat exchangers, which might provide insight into the boiling heat transfer performance of cross-ribbed geometries, are often kept proprietary. Consequently, little is generally known about the manner in which geometry, flow conditions, channel orientation and fluid properties interact to determine the flow regime and heat transfer. More information about the nature of the convective boiling process in these geometries would make it possible to more fully assess the advantages of using ribbed-plate geometries for evaporator applications.

The study described here was undertaken to experimentally explore the convective boiling heat transfer and two-phase flow behavior in a cross-ribbed channel. Experiments in this study were conducted using a special test section which permitted direct visual

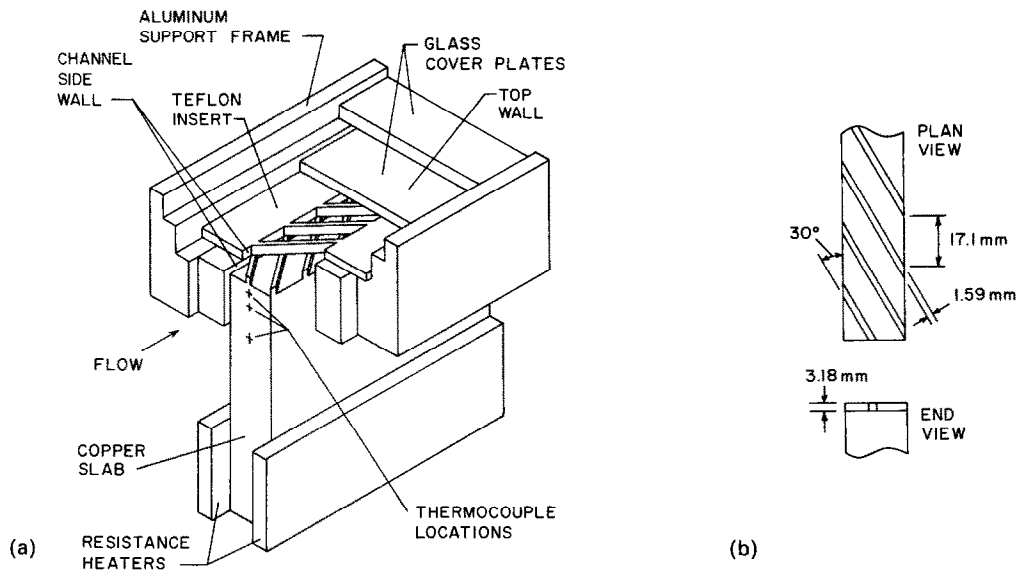

FIG. 1. (a) Cutaway view of test section; (b) drawing of rib geometry.

observation of the boiling process while simultaneously measuring the local heat transfer coefficient at several locations along the channel. One wall of the channel was heated while the opposite and lateral walls were adiabatic. Heating of a coolant channel on one side may arise in electronics cooling and other applications. Although the experiments are for one-sided heating, the results also provide insight into the boiling mechanisms which occur when both sides are heated.

This study specifically examined the effects of channel orientation on the boiling heat transfer and two-phase flow in the channel. Measured values of the local heat transfer coefficient are presented for saturated flow boiling of methanol and n-butanol at atmospheric pressure with the channel oriented vertically and in horizontal positions with top heating, side heating, and bottom heating of the channel. The observed two-phase flow behavior and dryout characteristics are described, and a method of correlating the convective boiling heat transfer data is also discussed.

EXPERIMENTAL APPARATUS AND PROCEDURE

Experimental studies of convective boiling in a cross-ribbed channel geometry were conducted using the test section shown in Fig. 1. One end of the rectangular copper slab shown in Fig. 1 was machined to form parallel ribs oriented at a 30° angle to the flow direction. These ribs have a rectangular cross-section, which is an idealization of the more rounded ribs usually found in ribbed-plate heat exchangers. The dimensions and spacing of the ribs are shown in Fig. 1. Ribs with the same dimensions and spacing were also machined in a Teflon sheet. This Teflon insert and the copper slab fit into the assembly shown in Fig. 1 to form a channel with cross-ribbed walls.

The side walls of the channel are Teflon to minimize lateral heat loss, and the inner glass plate on top of the Teflon insert forms the top wall of the channel to permit visual observation of the boiling process all along the channel. A second glass plate covers the inner one and as shown in Fig. 1 to reduce heat losses from the top of the assembly. The channel formed by the Teflon side walls, inner glass plate and copper slab is 1.91 cm wide, 6.4 mm high and 45.7 cm long. The hydraulic diameter based on the heated perimeter for this geometry, d_{hp}, is 12.1 mm, and the hydraulic diameter based on the wetted perimeter, d_h, is 5.2 mm.

The copper slab was heated at the bottom end by two electrical resistance heaters, which provide a virtually uniform heat input along the length of the channel. Heat is conducted from the heaters along the copper slab to the ribbed surface where it is transferred to the fluid in the channel. The back of the copper slab and heater assembly was completely enclosed in insulation so that heat leakage to the surroundings was negligible.

At 11.4, 22.9 and 34.3 cm downstream of the channel inlet, thermocouples were embedded in the copper slab, as indicated in Fig. 1, to determine the temperature gradient and surface temperature at three locations along the length of the channel. Small diameter thermocouples (0.9 mm beads) were installed in precisely located 1.0 mm diameter holes drilled into the centerline of the copper slab. The spacing between the first and third thermocouples was sufficiently large (19 mm) that uncertainty in the bead location was small compared to the separation distance. A least-squares fit of a linear relation to the three thermocouple readings was used to determine the temperature gradient in the slab and the surface temperature (between ribs) of the copper wall in contact with the fluid. Generally, all three points agreed closely with the curve-fit straight-line relation.

The temperature gradient determined from the slope of the linear relation fit to the thermocouple readings was used to calculate the heat flux to the ribbed surface of the channel. In both the single-phase and flow boiling experiments conducted in this study, the measured temperatures in the copper slab indicate that in the region near the ribbed surface, the temperature gradient along the channel (in the streamwise direction) was always much less than the temperature gradient normal to the channel wall. Consequently, at locations where single phase or convective boiling heat transfer coefficients were measured, conduction of heat upstream or downstream in the slab had no significant effect on the accuracy of the channel wall heat flux determined from the thermocouple measurements.

Thermocouples were also installed through the channel wall at the three locations noted above to measure the local fluid temperature. This result was combined with the calculated heat flux and surface temperature to compute the local heat transfer coefficient. Thermocouples in the test section were read using an Omega two-pole selector switch and a precision Fluke digital readout with a resolution of $\pm 0.06°C$. With this configuration, the uncertainty in the heat flux is estimated to be $\pm 6\%$ and the uncertainty in the heat transfer coefficients is estimated to be $\pm 11\%$.

A steady flow of liquid was supplied to the test section by the system shown schematically in Fig. 2. The power to the auxiliary heaters in the reservoir and the condenser water flow rate could be varied to control the temperature of the liquid at the inlet to the test section. The flow rate to the test section was set using the flow control valve shown in Fig. 2.

The liquid flow rate to the test section was measured using a Cole–Parmer rotameter. This flow meter was calibrated at several liquid temperatures so that the effect of property variation with temperature was taken into account. Rotameter calibration curves were determined for both fluids tested here.

Prior to running the heat transfer experiments, the ribbed-copper surface was cleaned with a mild acid solution and then thoroughly rinsed before filling the system with the test liquid. This procedure kept the ribbed-copper surface clean and free of tarnish throughout the test program.

Although Fig. 1 depicts the test section channel horizontally, the experiments reported here were done with the channel in both the vertical and horizontal positions. Power to the heaters in the test section was provided by two rheostats, which could be adjusted to control the heat input to the channel. Photographs of the two-phase flow at various locations along the channel were taken using a Pentax 35 mm camera with a 50 mm macro lens and an automatic strobe flash unit. The strobe unit provides flash pulses as short as 0.0001 s to freeze the very rapid motion of the two-phase flow.

Before running the convective boiling experiments,

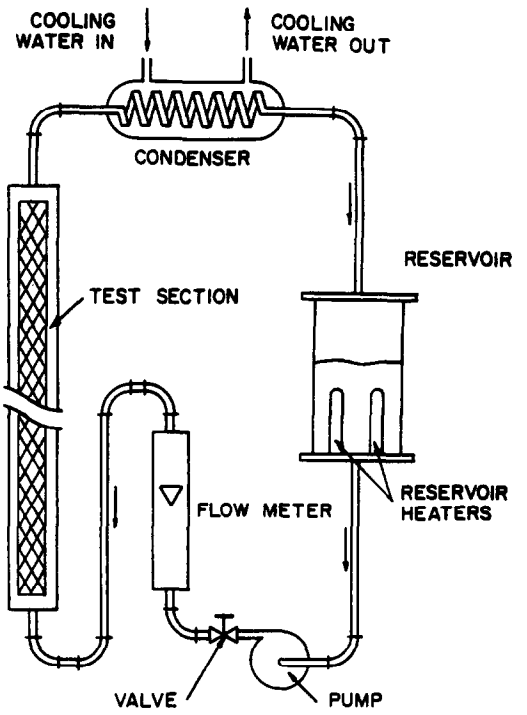

FIG. 2. Test system used in convective boiling experiments.

the single-phase heat transfer characteristics were first determined for the cross-ribbed channel in the test section. Local heat transfer coefficients were measured at low heat flux and high inlet subcooling where no vaporization occurs. After setting the flow rate and power to the heaters at the desired levels, the system was allowed to stabilize for 10–15 min before readings were taken. The resulting single-phase heat transfer data are plotted in non-dimensional form in Fig. 3. The heat transfer coefficients represented in this figure were measured at a specific downstream location and they are average values over the heated perimeter of the channel at that location.

The ribs on the copper surface will function as fins during the heat transfer process. In determining the heat transfer coefficient, the contribution of the rib surface area to the total surface area was therefore multiplied by the fin efficiency of the ribs to account

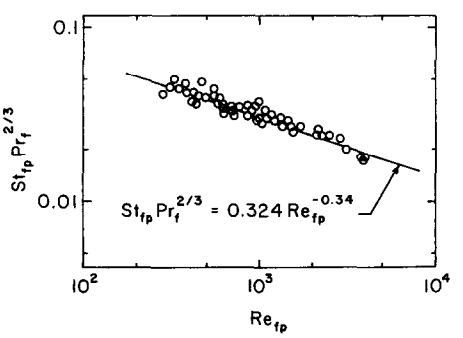

FIG. 3. Single-phase heat transfer data for channel.

for the slight difference between the rib temperature and the temperature of the wall between the ribs. The heat transfer coefficient determined in this way corresponds to the mean value over the perimeter of the channel which would result if the ribs and the wall between them were all at the same temperature. These values of h were iteratively calculated from the energy balance relation

$$W_c L_c k_c \nabla T_c = h(A_P + \eta_R A_R)(T_W - T_M) \quad (1)$$

where ∇T_c is the measured local temperature gradient in the copper and η_R is the fin efficiency of the ribs given by

$$\eta_R = \frac{1}{M(H+t/2)}\left[\frac{\tanh(MH)+h/k_c M}{1+(h/k_c M)\tanh(MH)}\right],$$
$$M = \sqrt{(2h/k_c t)}. \quad (2)$$

The correlation shown in Fig. 3 is a least-squares fit to the data. This single-phase heat transfer correlation will be discussed further in connection with the boiling heat transfer data.

For the flow boiling experiments, the system was allowed to stabilize at the selected power and flow settings before flow visualization photographs or data were taken. The thermocouple readings and liquid flow rates were recorded in the same manner as for the single-phase data. The downstream location where saturated nucleate boiling first began was also determined by visually inspecting the flow in the channel. This zero-quality point was taken to be the first downstream location where continuous growth and release of vapor bubbles occurred, and vapor bubbles were present throughout the liquid flow in the channel.

Thermocouple measurements of temperatures in the copper slab indicate that the heat flux varies somewhat along the channel wall near the location of the onset of boiling. Because thermocouples in the slab determine the heat flux at just a few locations, the exact nature of the variation is not known in this region, and, consequently, exact prediction of the zero-quality location from an energy balance is not possible. Approximate energy balances over this portion of the channel predict locations for the zero-quality point which are very close to the visually observed locations. However, due to the approximate nature of these energy balances, the visually observed locations are taken to be more accurate. Furthermore, comparisons indicate that the slight differences between the zero-quality locations obtained by these two methods generally correspond to an uncertainty of less than $\pm 6\%$ in the quality at the downstream location where flow boiling heat transfer coefficients were determined.

The heat transfer coefficient was determined at the two thermocouple locations near the downstream end of the channel where boiling was observed to occur. As for single-phase flow, the local heat transfer coefficient was obtained by iteratively solving equations (1) and (2) using the measured data at the location of interest. The only difference was that in equation (1), T_M was equal to T_{SAT}, the saturation temperature of the coolant. The boiling heat transfer coefficients calculated in this manner are average values over the heated perimeter of the channel.

The mass flux, G, was determined from the flow meter reading and the geometry of the channel. The quality at the thermocouple locations was determined by using the measured heat input values in an energy balance over the portion of the channel where saturated boiling occurred. The measurements thus indicated the value of h_{tp} which corresponded to specific values of x and G.

Values of h_{tp} were determined for convective boiling of methanol and n-butanol at or near atmospheric pressure. Four different channel orientations were tested. Data have been obtained for values of quality and mass flux in the ranges $0.05 < x < 0.8$ and $5 < G < 90$ kg m^{-2} s^{-1}. Although the values of mass flux considered in these experiments are relatively low, mass flux levels between 20 and 90 kg m^{-2} s^{-1} are commonly encountered in evaporators for small refrigeration and air-conditioning systems, and other thermal control applications in which a low evaporator pressure drop is desirable. Hence, the results of these experiments relate most directly to applications of this type. The estimated uncertainty in the measurements is $\pm 5\%$ for G, $\pm 9\%$ for x and $\pm 13\%$ for h_{tp}.

RESULTS FOR VERTICAL FLOW

During vertical-flow convective boiling, the flow appeared to be in the bubbly regime very near the location of the onset of saturated boiling. A very short distance downstream, the flow had undergone a transition to slug flow, and a short distance thereafter, the transition to churn or annular flow was observed. A rapid transition from bubbly flow to an annular flow configuration was characteristic of the boiling processes for both fluids tested here.

A photograph of the annular two-phase flow observed during vertical-flow convective boiling of methanol is shown in Fig. 4. At the thermocouple location indicated by the arrow, $G = 15.1$ kg m^{-2} s^{-1}, $x = 0.28$ and $h_{tp} = 7.55$ kW m^{-2} K^{-1}. The liquid film traveling upward along the front (glass) wall and back (heated) wall appeared to follow the rib pattern diagonally upward and across the channel, until it hit the side wall. The liquid then appeared to transfer to the opposite (front or back) wall and flowed diagonally upward and across the channel in the opposite direction. This produced an almost helical motion of the liquid film in the channel.

Intermittently, waves could sometimes be observed to travel upward in the liquid film along the front and back walls of the channel. However, these waves were usually broken up and dissipated in a very short distance because of the presence of the ribs. The annular

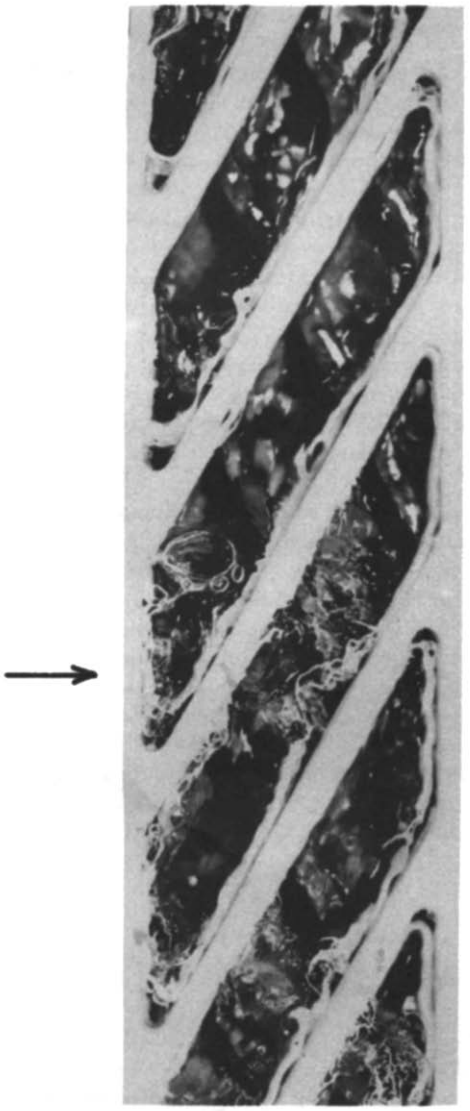

FIG. 4. Photograph of annular film flow boiling of methanol in a vertical cross-ribbed channel at $G = 15.1\ \text{kg m}^{-2}\text{s}^{-1}$ and $q'' = 55.5\ \text{kW m}^{-2}$. At the thermocouple location indicated by the arrow, $x = 0.28$ and $h_{tp} = 7.55\ \text{kW m}^{-2}\text{K}^{-1}$.

flow behavior observed during convective boiling of n-butanol was very similar to that observed for methanol.

In the churn and annular flow regimes, virtually no nucleate boiling was visually observed during the convective boiling experiments, even though the wall superheat was often over 9°C. In Fig. 4, very little, if any, evidence of nucleate boiling can be seen. During the experiments, bubbles could be observed at a few locations in the corner where the rib meets the copper surface. The liquid film is thicker and the convective component of heat transport is expected to be weaker in these corner regions. Consequently, there will be less tendency to suppress nucleation there. Hence, it is not surprising that nucleation persists at a few points in these corner locations, even though it has been thoroughly suppressed along the flat surfaces of the channel.

The vertical flow conditions at which data were obtained are indicated on a flow regime map of the type proposed by Hewitt and Roberts [5] for upward co-current flow in Fig. 5. It can be seen that the flow conditions studied here span the transition from churn flow to annular flow. The transition line suggested by Hewitt and Roberts [5] corresponds approximately to $\rho_g j_g^2 = 200$ for the range of $\rho_f j_f^2$ encountered in our experiments. This would place all of our data in the churn flow regime. For the flows considered here, the transition condition suggested by Wallis [6] is lower, but it would also place much of our data in the churn flow regime.

For virtually all of our vertical flow data, our visual observations indicated that the flow in the channel was annular in configuration. For about half of the data points, the flow appeared slightly oscillatory in nature, with visible intermittent downflow of liquid. For these circumstances, which were usually observed at lower qualities, the flow looked more like churn flow than steady annular flow. The other half of our data appeared to be in upward annular flow.

Based on our visual observations, the approximate transition line between churn and annular flow is indicated in Fig. 5. In terms of the j_g^* parameter defined by Wallis [6], the transition conditions observed during these flow boiling experiments correspond approximately to $j_g^* = 0.4$.

The experimentally determined variations of h_{tp} with x for various G values are shown in Figs. 6(a) and (b) for methanol and n-butanol, respectively. The variation of h_{tp} with x is shown for low to moderate values of G in these plots. Additional data were obtained for higher values of G, but the systematic variation of h_{tp} with x was not determined. The measured value of h_{tp} is seen to increase with increasing G and x for both fluids. The data obtained at higher mass flux levels were consistent with the trends

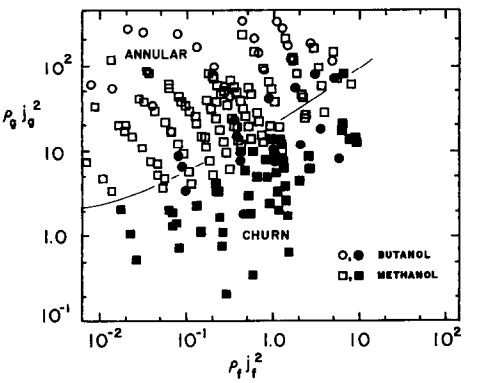

FIG. 5. Visually observed two-phase flow regimes during convective boiling in a vertical cross-ribbed channel. The open and solid symbols correspond to annular flow and churn flow, respectively. The curve denotes the approximate transition based on visual observations.

observed in Figs. 6(a) and (b). The variations of h_{tp} with x and G shown in these figures are qualitatively similar to those obtained by Carey and Mandrusiak [7] for a vertical channel with offset strip fins.

In addition to the experimental data, Figs. 6(a) and (b) also show the variation of the convective boiling heat transfer coefficient predicted by the Bennett and Chen [8] correlation for a vertical round tube with the same hydraulic diameter as the channel used in our experiments (d_h = 5.2 mm). The variation of h_{tp} with x was calculated using the Bennett and Chen [8] correlation for the wall temperatures and mass flux levels measured in our experiments. Due to the more complicated nature of the cross-ribbed geometry, the data for this channel configuration would not generally be expected to agree with predictions of the Bennett and Chen [8] correlation. The purpose of presenting the variation of h_{tp} predicted by the Bennett and Chen [8] correlation is to compare the heat transfer performance characteristics of the cross-ribbed channel with those of a round tube under similar conditions. It can be seen in Figs. 6(a) and (b) that for the same G and x values, the heat transfer coefficients for the ribbed channel are as much as three times those for the round tube.

Calculations using the Bennett and Chen [8] correlation also indicate that a substantial nucleate boiling effect on heat transfer would exist in the round tube, even for conditions resulting in annular flow. In contrast, we observed virtually no nucleate boiling in the ribbed channel when the flow is in the annular flow regime. It appears that for nominally the same annular flow conditions, the ribbed channel suppresses nucleate boiling more effectively than a round tube with the same hydraulic diameter.

Based on an approximate model of transport in the liquid film, Carey and Mandrusiak [7] derived the following correlation for annular film-flow boiling in a partially-heated vertical channel:

$$\Psi = \left(\frac{h_{tp}}{h_{fp}}\right) \times \frac{4.74\sqrt{A}\tan^{-1}[0.149\sqrt{(Re_{fp}\,Pr_f)}\sqrt{(d_h/d_{hp})}]}{Re_{fp}^{n/2}\,Pr_f^{1/6}(d_{hp}/d_h)^{n/2}} \quad (3a)$$

$$= \left[1 + \frac{20}{X_{tt}} + \frac{1}{X_{tt}^2}\right]^{1/2} \quad (3b)$$

where n and A are constants from the single-phase heat transfer correlation for turbulent flow

$$St_{fp}\,Pr_f^{2/3} = A\,Re_{fp}^{-n} \quad (4)$$

and X_{tt} is given by equation (10).

The geometry of the channel studied here is considerably different from the partially-heated channel of rectangular cross-section considered by Carey and Mandrusiak [7]. However, for annular film flow, the liquid film is often very thin, and large-scale variations of the channel wall geometry may have only a weak effect on local transport. It may therefore be possible to also correlate the heat transfer data for this geometry in terms of X_{tt} and Ψ as defined above.

The measured heat transfer data obtained here for vertical flow boiling of methanol and n-butanol are plotted in terms of Ψ and $1/X_{tt}$ in Figs. 7(a) and (b), respectively. In these figures, the open symbols indicate annular flow and the solid symbols indicate churn flow. In calculating Ψ for the data in these figures, the values of n and A were taken from the correlation in Fig. 3 to be 0.34 and 0.324, respectively. Also shown in Figs. 7(a) and (b) is the curve corresponding to equation (3b).

It can be seen in Figs. 7(a) and (b) that for both fluids tested here, the data correlate well in terms of Ψ and X_{tt} over wide ranges of mass flux and quality. Even the data for vertical churn flow are consistent with the annular flow trend. However, for both methanol and butanol, the heat transfer data are consistently about 20% higher than the Ψ variation predicted by equation (3). Actually, there is no reason, *a priori*, to believe that equation (3) should fit the data for this geometry. However, as shown in Figs. 7(a) and (b), the data for this geometry agree well with the

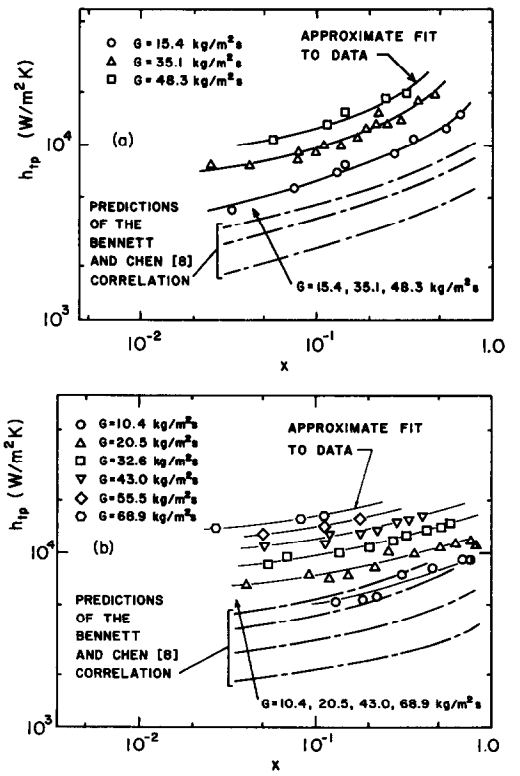

FIG. 6. Measured local heat transfer coefficients for convective boiling in a partially heated vertical cross-ribbed channel. Data shown are for (a) methanol and (b) n-butanol. The half filled symbols denote partial dryout of the heated surface.

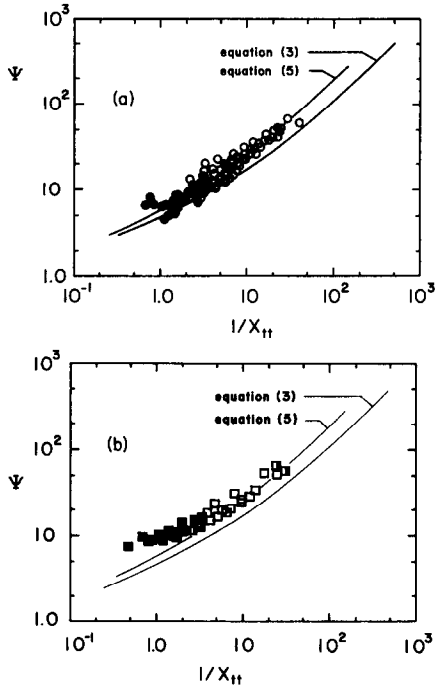

FIG. 7. Comparison of the measured heat transfer data for convective boiling in a vertical cross-ribbed channel with correlation (3) proposed by Carey and Mandrusiak [7] and equation (5). Data shown are for (a) methanol and (b) n-butanol. The solid symbols and open symbols denote churn flow and annular flow, respectively. Half filled symbols denote partial dryout of the heated surface.

relation

$$\Psi = \left[1 + \frac{30}{X_{tt}} + \frac{3.0}{X_{tt}^2}\right]^{1/2}. \quad (5)$$

Data in the annular flow regime agree very well with equation (5) for both fluids tested here. Even for data in the churn flow regime, agreement with equation (5) is quite good, although the scatter about the curve is a bit larger in some cases.

RESULTS FOR HORIZONTAL FLOW

During horizontal-flow convective boiling, the flow was observed to be in the bubbly regime very near the location of the onset of saturated boiling. A very short distance downstream, the flow had undergone a transition to slug flow, and a short distance thereafter, the transition from slug flow to stratified, wavy or annular flow was observed. Because of the rapid transition to one of these three regimes, all of our measured heat transfer data for horizontal flow are in the stratified, wavy or annular flow regime.

For horizontal flows in the stratified, wavy and annular flow regimes, virtually no nucleate boiling was visually observed during the convective boiling experiments, even though the wall superheat was often over 10°C. As in the vertical experiments, bubbles could be observed at a few locations in the corner where the rib meets the copper surface. The same weaker tendency to suppress nucleation in these corner regions apparently exists in both vertical and horizontal flows.

The horizontal flow conditions at which heat transfer measurements were made are indicated on a flow regime map of the type proposed by Taitel and Dukler [9] for horizontal co-current flow in Fig. 8. The flow conditions studied here resulted in stratified, wavy or annular flow. Note that data for side and bottom heating are shown. For the same conditions, the flow behavior for top heating was virtually the same as for bottom heating.

The transition from wavy to annular flow is observed in the upper part of Fig. 8 where the data for wavy and annular flow are plotted in terms of X_{tt} and F. Here, X_{tt} is the Martinelli parameter for turbulent–turbulent flow

$$X_{tt} = [(dp/dz)_{Ff}/(dp/dz)_{Fg}]^{1/2} \quad (6)$$

and F is defined as

$$F = \left[\frac{\rho_g j_g^2}{(\rho_f - \rho_g) d_h g}\right]^{1/2}. \quad (7)$$

The single-phase pressure gradients in equation (6) are evaluated as

$$(dp/dz)_{Ff} = -\frac{2 f_f G^2 (1-x)^2}{\rho_f d_h} \quad (8a)$$

$$(dp/dz)_{Fg} = -\frac{2 f_g G^2 x^2}{\rho_g d_h}. \quad (8b)$$

In equations (8a) and (8b), the single-phase friction factors are determined using the modified Reynolds analogy with the heat transfer correlation determined

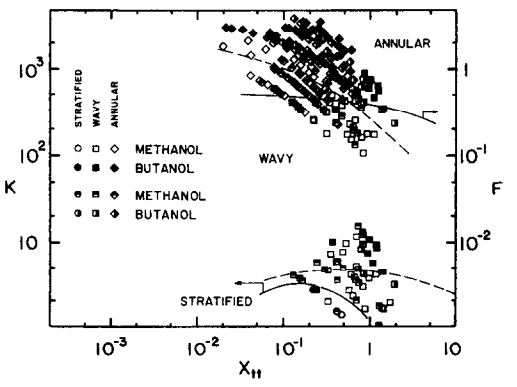

FIG. 8. Visually observed two-phase flow regimes during convective boiling in a horizontal cross-ribbed channel. The open and solid symbols correspond to bottom heating and the half filled symbols correspond to side heating. The solid curves denote the approximate transitions based on visual observations. The broken curves are the transitions proposed by Taitel and Dukler [9] for horizontal flow in a round tube.

experimentally for turbulent flow in this geometry

$$f_f/2 = St_f\, Pr_f^{2/3} = A\, Re_f^{-n} \tag{9a}$$

$$f_g/2 = St_g\, Pr_g^{2/3} = A\, Re_g^{-n}. \tag{9b}$$

The single-phase friction factor determined in this way is not the same as that for the entire cross-ribbed matrix, which includes the effect of form drag on the ribs. The modified Reynolds analogy relation accounts only for the fluid shear on the channel walls. Also, since the wall shear acts around the entire channel perimeter, the hydraulic diameter based on heated perimeter in the heat transfer correlation is replaced by the hydraulic diameter based on the wetted perimeter.

Combining equations (6), (8) and (9), it can be shown that

$$X_{tt} = \left(\frac{\rho_g}{\rho_f}\right)^{1/2}\left(\frac{\mu_f}{\mu_g}\right)^{n/2}\left(\frac{1-x}{x}\right)^{1-n/2} \tag{10}$$

which is consistent with the definition of X_{tt} used by Carey and Mandrusiak [7] to correlate data for vertical flows in offset strip fin geometries. Equation (10) with $n = 0.34$ was used to calculate X_{tt} for the experimental data shown in Fig. 8.

The curve in the upper portion of Fig. 8 indicates the approximate location of the transition from wavy to annular flow based on visual observations. This transition is approximately the same as that proposed by Taitel and Dukler [9] for horizontal flow in more conventional channel configurations. However, for the cross-ribbed geometry, the exact location of the transition is slightly different.

The transition from stratified to wavy flow is observed in the lower portion of Fig. 8, where the data for stratified and wavy flow are plotted in terms of X_{tt} and K. Here, K is defined as

$$K = \left[\frac{\rho_g j_g^2 j_f}{g(\rho_f - \rho_g)\nu_f}\right]^{1/2}. \tag{11}$$

As seen in Fig. 8, only a few points correspond to stratified flow. Stratified flow could be achieved only at very low flow rates, apparently because agitation of the flow by the ribs serves to trip the flow into a wavy flow mode. The curve in the lower portion of Fig. 8 indicates the approximate location of the flow regime transition, based on visual observation. Because we have only a few points in the stratified regime, this placement of the transition line is somewhat tentative. It is interesting to note, however, that the indicated transition from stratified to wavy flow is only slightly different from that proposed by Taitel and Dukler [9] for horizontal flow in a round tube.

The experimentally determined variations of h_{tp} with x for various G values are shown in Figs. 9 and 10 for the horizontal channel orientations tested here. All the data shown are for saturated convective boiling of methanol or n-butanol at or near atmospheric pressure. The variation of h_{tp} with x is shown for low

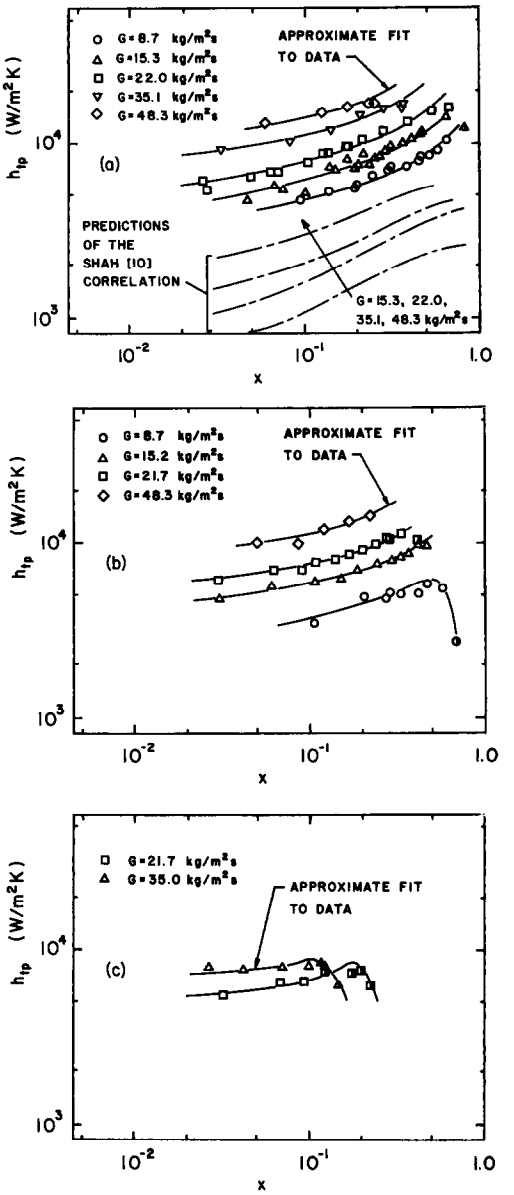

FIG. 9. Measured local heat transfer coefficients for convective boiling of methanol in a partially heated horizontal channel. Data shown are for (a) bottom heating, (b) side heating and (c) top heating. The half filled symbols denote partial dryout of the heated surface.

to moderate values of G in these plots. As for the vertical tests, additional data were obtained for higher values of G, but the systematic variation of h_{tp} with x was not determined.

The convective boiling heat transfer data for horizontal flow of methanol and n-butanol with bottom heating are shown in Figs. 9(a) and 10(a), respectively. A close comparison of Figs. 9(a) with 6(a), and 10(a) with 6(b) reveals that for the same quality and mass flux, the measured heat transfer coefficients for vertical and bottom-heated horizontal flow are virtually the same. The same trends of increasing h_{tp} with G

and x seen in the vertical data are also apparent in Figs. 9(a) and 10(a).

In addition to the experimental data, Fig. 9(a) also shows the variation of the convective boiling heat transfer coefficient predicted by the Shah [10] correlation for a horizontal round tube with the same hydraulic diameter as the channel used in our experiments. The variation of h_{tp} was calculated using the Shah [10] correlation for the heat flux values measured in our experiments, at mass flux values of 15.3, 22.0, 35.1 and 48.3 kg m^{-2} s^{-1}.

For horizontal flow, the Shah [10] correlation accounts for the fact that the upper portion of the tube wall may be at least partially dry. Consequently, the average value of h_{tp} predicted by this correlation may be somewhat lower than that for the bottom portion of the channel alone. However, even if the top half of the round tube were totally dry, the heat transfer coefficient over the lower wetted half of the wall would only be twice the average value predicted by the Shah [10] correlation. It can be seen in Fig. 9(a) that, for comparable conditions, the heat transfer coefficient for the ribbed channel is as much as five times that for a round tube. Even allowing for partial dryout of the round tube, the h_{tp} values for the bottom of the ribbed channel are significantly higher than corresponding values for the bottom of a round tube.

Figures 9(b) and 10(b) show convective boiling heat transfer data for horizontal flow with the channel rotated 90° so that heat is applied to one side wall of the channel. By comparing Fig. 9(b) with Figs. 9(a) and 6(a), and Fig. 10(b) with Figs. 10(a) and 6(b), it can be seen that at the same x and G values, the measured heat transfer coefficients for $G > 10$ kg m^{-2} s^{-1} are virtually the same as for the vertical and bottom-heated horizontal flows. At high mass flux, the disturbance of the flow by the ribs apparently helps to distribute liquid all over the channel walls, despite the tendency of gravity to pull liquid into the bottom portion of the channel. However, for methanol at $G = 8.7$ kg m^{-2} s^{-1}, the heat transfer coefficient is seen to drop precipitously at high quality. At this low mass flux, the mixing of the flow by the ribs is not adequate to keep the entire heated surface wet at high quality. The heated wall thus became partially dry at moderate quality, resulting in a low average heat transfer coefficient. It appears, therefore, that this geometry performs as well in this orientation as for vertical flow, provided the mass flux is not too low.

A limited amount of heat transfer data for top-heated horizontal flow of methanol is shown in Fig. 9(c). In the top-heated experiments, the heated surface was observed to begin drying-out at very low quality. This is reflected in Fig. 9(c) as the roll-over in the heat transfer data with increasing x which occurs between $x = 0.1$ and 0.2. Apparently this cross-ribbed geometry does not effectively transfer liquid across the narrow dimension of the channel, even at low to moderate quality, when gravity opposes the transfer. Consequently, it is difficult to keep the top wall of the channel wet in this orientation, and early dryout may greatly reduce the heat transfer coefficient on the top wall. Because of this early dryout behavior, only a small amount of data for methanol at low quality was obtained for this orientation.

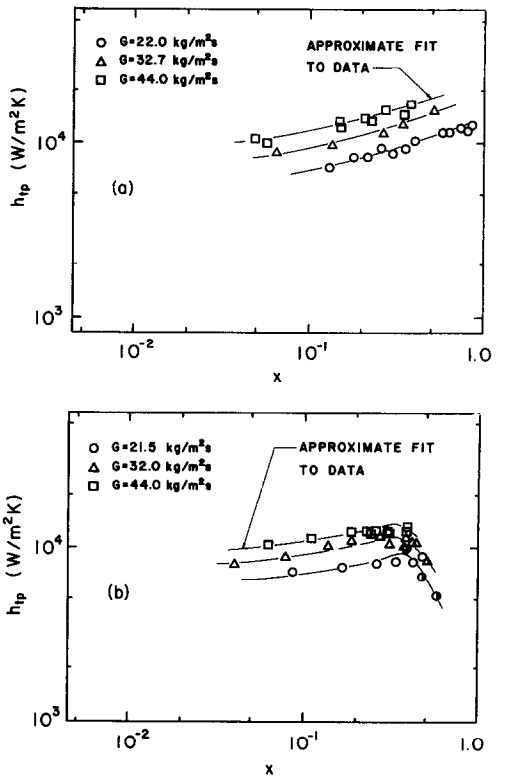

FIG. 10. Measured local heat transfer coefficients for convective boiling of n-butanol in a partially heated horizontal channel. Data shown are for (a) bottom heating and (b) side heating. The half filled symbols denote partial dryout of the heated surface.

For horizontal annular flow, gravitational effects may be weak, and transport in the liquid film may be similar to that for vertical flow at the same flow conditions. Since the vertical data correlated well in terms of the X_{tt} and Ψ parameters defined by Carey and Mandrusiak [7] for vertical annular flow, the horizontal data may also be expected to correlate well in terms of these parameters, at least for conditions corresponding to annular flow.

The measured heat transfer data obtained for bottom-heated and side-heated horizontal flow are plotted in terms of Ψ and $1/X_{tt}$ in Figs. 11(a) and (b). The little data obtained for top heating is not shown, since it is all for low quality conditions corresponding to bubbly or wavy flow. In these figures, data corresponding to partial dryout of the heated surface are denoted by half filled symbols. As for the vertical flow data, the values of n and A from the single phase correlation shown in Fig. 3 were used to calculate Ψ and X_{tt} for the data in Figs. 11(a) and (b). Also shown

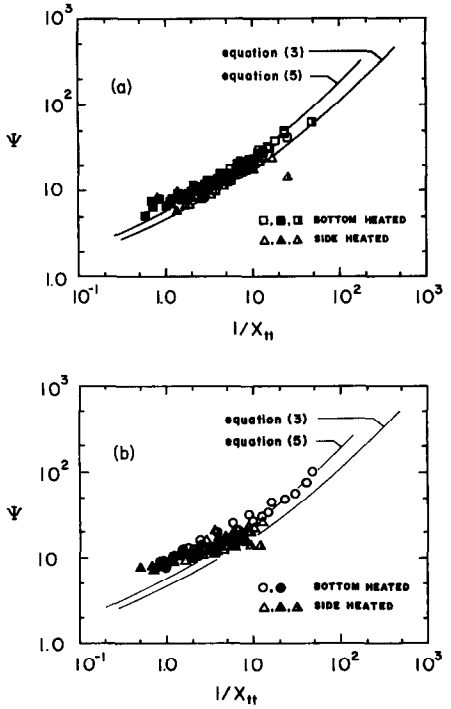

FIG. 11. Comparison of the measured heat transfer data for convective boiling in a horizontal cross-ribbed channel with correlation (3) proposed by Carey and Mandrusiak [7] and equation (5). Data shown are for (a) methanol and (b) n-butanol. The solid symbols and open symbols denote wavy flow and annular flow, respectively. The half filled symbols denote partial dryout of the heated surface.

in these figures are curves corresponding to equations (3b) and (5).

It can be seen in Figs. 11(a) and (b) that for both side heating and bottom heating, the data correlate well in terms of Ψ and X_{tt} over wide ranges of mass flux and quality. Even the data for wavy flow are consistent with the annular flow trend. The only exceptions are the partial dryout data for side heating, which are slightly low relative to the trend in the other data. As for the vertical results, the heat transfer data in Figs. 11(a) and (b) are consistently about 20% higher than the correlation given by equation (3). However, these horizontal data are seen to agree well with the correlation given by equation (5). The annular flow data for both methanol and n-butanol agree very well with equation (5) for both horizontal orientations represented in Fig. 11. Even for data in the wavy flow regime, agreement is quite good, although scatter about the curve is a bit larger. Hence, the correlation given by equation (5) fits both the vertical flow and horizontal data, for churn, wavy or annular flow conditions, provided that the heated surface is fully wetted by the liquid film.

CONCLUSIONS

Measurements of local heat transfer coefficients and observations of the two-phase flow in this study reveal a number of interesting features of convective boiling in a partially-heated cross-ribbed channel. Visual observations indicated that for the relatively low pressure conditions studied here, the two-phase flow for a vertical channel takes on an annular configuration a short distance downstream of the beginning of saturated boiling. Beyond that point, the vertical flows studied here were in either the churn flow or annular flow regime. Similarly, for horizontal flows, the two-phase flow was found to be in either a wavy flow or annular flow regime a short distance downstream of the onset of saturated boiling. In these regimes, nucleate boiling was suppressed over virtually the entire heated surface and the phase change was accomplished primarily by convection of heat to the liquid–vapor interface where evaporation occurred.

For vertical two-phase flow in the rib geometry tested here, the transition from churn flow to annular flow was found to occur at a slightly lower value of $\rho_g j_g^2$ than values suggested by Hewitt and Roberts [5] or Wallis [6] for vertical round tubes. For horizontal flows, the transition from wavy to annular flow was found to occur at about the same values of F as for horizontal flow in round tubes, although the exact location and slope of the transition line were somewhat different. Although the data obtained for stratified flow is limited, the results indicate that the transition from stratified to wavy flow in the cross-ribbed channel occurs at about the same conditions as for horizontal flow in round tubes.

For both horizontal and vertical flows, the measured value of the local convective boiling heat transfer coefficient was found to increase as quality or mass flux increases, in a manner similar to that for round tubes. For horizontal flow with bottom or side heating, the measured heat transfer coefficient was virtually the same as for vertical flow. The only exceptions to this rule were at low mass flux for side heating. For these conditions, the ribs failed to distribute liquid over the entire heated surface, resulting in local dryout of the heated surface and a subsequent drop in the local heat transfer coefficient.

For convective boiling in a vertical cross-ribbed channel, it was also found that the measured convective boiling heat transfer coefficient can be two to three times larger than the value predicted by the Bennett and Chen correlation [9] for convective boiling in a vertical round tube with the same hydraulic diameter, mass flux, quality, and wall temperature. Furthermore, the Bennett and Chen correlation predicts a strong nucleate boiling contribution to the overall heat transfer in comparable round tube flows. In contrast, we found virtually no nucleate boiling in the ribbed channel flow under comparable conditions. Apparently the enhancement of the forced convection effect caused by the ribs also results in a stronger suppression of nucleate boiling.

For horizontal flow with top heating, the measured heat transfer coefficients at very low quality were consistent with the data obtained for vertical flow. How-

ever, in this orientation, transfer of liquid to the top wall of the channel against gravity was poor, even at low quality and moderate mass flux. Consequently, at low quality ($x \simeq 0.10$) the heated top wall of the channel began to dry out, and the heat transfer coefficient dropped off rapidly with increasing quality. Although this channel geometry provides superior performance in a vertical orientation, for horizontal flow with top heating, early dry-out may seriously degrade performance.

The heat transfer data obtained here for vertical flow in the churn flow and annular flow regimes were found to correlate very well in terms of the modified Martinelli parameter (X_{tt}) and Ψ parameter proposed by Carey and Mandrusiak [7]. The data for horizontal flow with side heating or bottom heating in the wavy and annular flow regimes also correlated well in terms of these parameters. A single correlation for Ψ as a function of X_{tt} was found to fit all the data for these three configurations. This relation may be a useful starting point for development of a general correlation technique for predicting convective boiling heat transfer performance of cross-ribbed channels. However, at the present time, more data for other geometries is needed to fully assess the usefulness of this approach.

Acknowledgements—The authors wish to acknowledge support for this research by the National Science Foundation under grant No. CBT-8451781. The assistance of Sue Bavonese and Ms Loris C.-H. Donahue in preparation of the manuscript is also appreciated.

REFERENCES

1. G. R. Kubanek and D. L. Miletti, Evaporative heat transfer and pressure drop performance of internally-finned tubes with refrigerant 22, *Trans. Am. Soc. Mech. Engrs*, Series C, *J. Heat Transfer* **101,** 447–452 (1979).
2. D. G. Thomas and G. Young, Thin film evaporation enhancement by finned surfaces, *Ind. Engng Chem. Proc. Des. Dev.* **9,** 317–323 (1970).
3. M. A. R. Akhanda and D. D. James, An experimental study of the relative effects of transverse and longitudinal ribbing of the heat transfer surface in forced convective boiling. In *Two-phase Heat Exchanger Symposium*, HTD-Vol. 44, pp. 83–90. ASME, New York (1985).
4. C. B. Panchal, D. L. Hillis and A. Thomas, Convective boiling of ammonia and Freon 22 in plate heat exchangers, *Proceedings of the ASME/JSME Thermal Engineering Joint Conference*, Vol. 2, pp. 261–268 (1983).
5. G. F. Hewitt and D. N. Roberts, Studies of two-phase flow patterns by simultaneous X-ray and flash photography, AERE Report AERE-M 2159, HMSO (1969).
6. G. B. Wallis, *One Dimensional Two-phase Flow*, Chap. 11. McGraw-Hill, New York (1969).
7. V. P. Carey and G. D. Mandrusiak, Annular film-flow boiling of liquids in a partially heated, vertical channel with offset strip fins, *Int. J. Heat Mass Transfer* **29,** 927–939 (1986).
8. D. L. Bennett and J. C. Chen, Forced convective boiling in vertical tubes for saturated pure components and binary mixtures, *A.I.Ch.E. Jl* **26,** 454–461 (1980).
9. Y. Taitel and A. E. Dukler, A model for predicting flow regime transitions in horizontal and near-horizontal gas–liquid flow, *A.I.Ch.E. Jl* **22,** 47–55 (1976).
10. M. M. Shah, A new correlation for heat transfer during boiling flow through pipes, *ASHRAE Trans.* **82,** 66–86 (1976).

TRANSFERT THERMIQUE ET ECOULEMENT DIPHASIQUE DANS UN CANAL AVEC AILETTES ET PARTIELLEMENT CHAUFFE

Résumé—Des données de transfert de chaleur et de visualisation d'un écoulement diphasique sont présentées pour l'ébullition de liquides saturés dans un canal avec ailettes semblable aux géométries utilisées dans les échangeurs compacts à plaques. Une section d'essai spéciale permet une visualisation directe du mécanisme d'ébullition pendant que le coefficient local de transfert thermique est mesuré en différents endroits le long du canal. Une paroi du canal est chauffée tandis que la paroi opposée et les côtés sont adiabatiques. Les coefficients de transfert mesurés localement sur la portion chauffée sont obtenus pour l'ébullition convective du méthanol et du *n*-butanol à la pression atmosphérique, avec orientation verticale ou horizontale, chauffage du canal au sommet, latéralement ou en partie inférieure. Pour le même réfrigérant et les mêmes conditions d'écoulement, depuis les qualités modérées jusqu'aux fortes, les coefficients de transfert thermique pour les orientations verticale et horizontale diffèrent assez peu. Par contre, pour ces orientations, l'assèchement partiel de la paroi chaude réduit le coefficient de transfert. On décrit une méthode pour mettre en formule les données de l'ébullition avec film annulaire dans les géométries étudiés.

WÄRMEÜBERGANG UND ZWEIPHASENSTRÖMUNG BEI KONVEKTIVEM SIEDEN IN EINEM TEILWEISE BEHEIZTEN, QUERBERIPPTEN KANAL

Zusammenfassung—Es wird über gemessene örtliche Wärmeübergangskoeffizienten und visuelle Beobachtungen von Zweiphasenströmungen bei konvektivem Sieden von gesättigten Flüssigkeiten in einem querberippten Kanal berichtet. Die Geometrie ist ähnlich der, wie sie bei Plattenkompaktwärmetauschern benutzt wird. Die Experimente in dieser Untersuchung wurden ausgeführt unter Benutzung einer speziellen Meßstrecke, die eine direkte visuelle Beobachtung des Siedevorgangs bei gleichzeitiger Messung des lokalen Wärmeübergangskoeffizienten an verschiedenen Orten entlang des Kanals erlaubte. Eine Wand des Kanals wurde beheizt, während die gegenüberliegende und die seitlichen Wände adiabat waren. Man erhielt gemessene örtliche Wärmeübergangskoeffizienten im beheizten Bereich der Kanalwand für konvektives Sieden mit Methanol und *n*-Butanol unter Atmosphärendruck bei senkrecht gestelltem Kanal oder waagerecht liegendem Kanal mit Beheizung der Grundfläche, einer Seitenfläche oder der Deckfläche. Bei vertikaler Anordnung wurde über den größten Teil der Kanallänge Schaum- oder Ringströmung beobachtet, während bei horizontaler Anordnung hauptsächlich Wellen- oder Ringströmung auftraten. Visuelle Beobachtungen zeigten, daß kein Blasensieden vorhanden war unter einer dieser drei Strömungsformen. Es ergab sich, daß für gleiche Kühl- und Strömungsbedingungen, bei mäßig hohem Massendampfgehalt, die gemessenen Wärmeübergangskoeffizienten für konvektives Sieden sich bei vertikaler und horizontaler Anordnung gewöhnlich nur um einen kleinen Betrag unterschieden. Jedoch wurde bei einigen Anordnungen manchmal örtliches 'dryout' der beheizten Kanalwand beobachtet; dies verringerte den Wärmeübergangskoeffizienten. Eine Methode zur Korrelierung der Wärmeübergangskoeffizienten für Ringfilm-Strömungssieden bei querberippten Kanalgeometrien wird ebenfalls beschrieben.

ТЕПЛООБМЕН И ДВУХФАЗНОЕ ТЕЧЕНИЕ ПРИ КИПЕНИИ В ЧАСТИЧНО ОБОГРЕВАЕМОМ КАНАЛЕ С ПОПЕРЕЧНЫМ ОРЕБРЕНИЕМ

Аннотация—Приводятся результаты измерения локального теплообмена и данные визуальных наблюдений двухфазного потока при кипении насыщенных жидкостей в канале с поперечным оребрением, имеющем конфигурацию, подобную используемой в компактных пластинчатых теплообменниках. Эксперименты проводились в специальной рабочей секции канала, которая позволяла непосредственно наблюдать кипение и одновременно измерять локальный коэффициент теплообмена по длине канала. Одна стенка канала нагревалась, а противоположная и боковые стенки были адиабатическими. Измерены локальные коэффициенты теплообмена на нагреваемых участках канала при движении кипящего метанола и н-бутанола при атмосферном давлении. Канал ориентировался вертикально и горизонтально, обогрев производился сверху, сбоку и снизу. Наблюдения показали, что в вертикальном положении преобладают вихревые и кольцевые течения, а в горизонтальных—волновые и кольцевые режимы течения почти по всей длине канала. Визуальные наблюдения также показали, что ни в одном из этих режимов не отмечалось пузырьковое кипение. При этом измеренные коэффициенты теплообмена при движении кипящих жидкостей в горизонтальных и вертикальных каналах для одного и того же теплоносителя и одинаковых режимах течения, а также при средних и высоких степенях объемного паросодержания отличались незначительно. Однако, при некоторых ориентациях наблюдалось, что частичное высыхание нагреваемой стенки канала иногда приводило к уменьшению коэффициента теплообмена. В работе также приводится метод обобщения данных по теплообмену при пленочном кипении и кольцевом режиме течения в поперечно оребренных каналах.